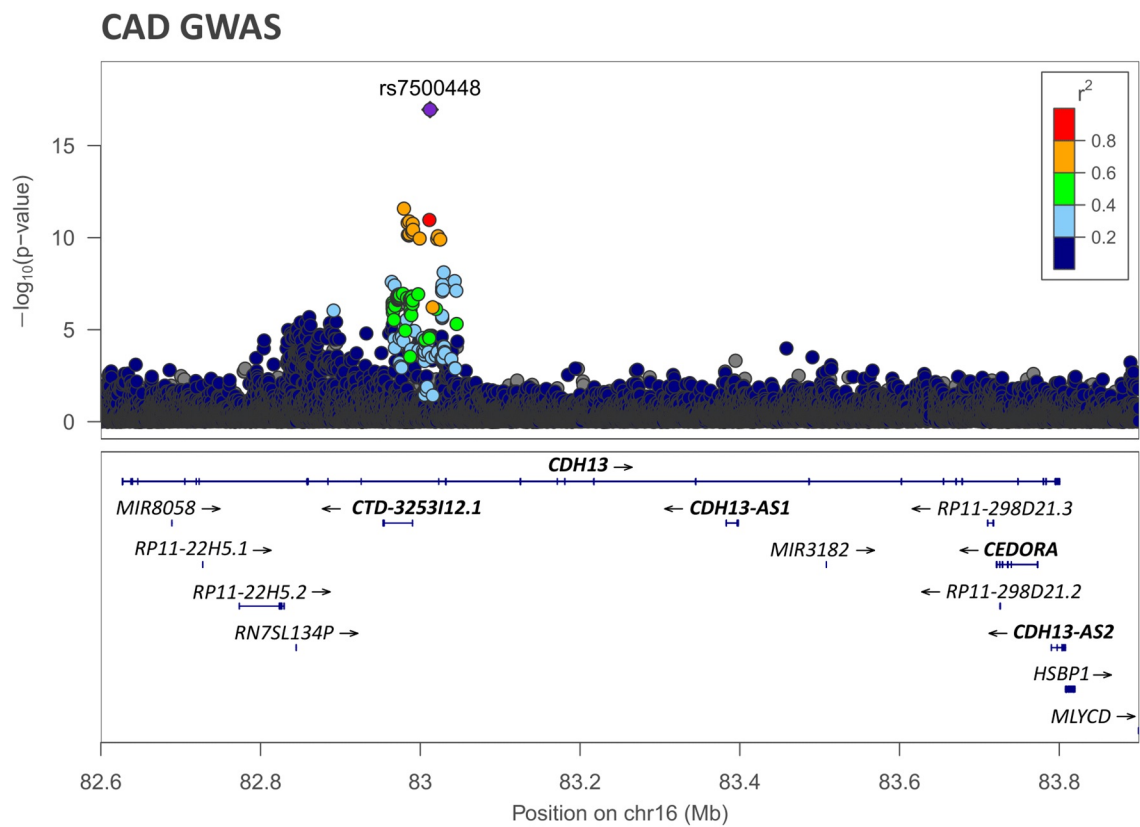
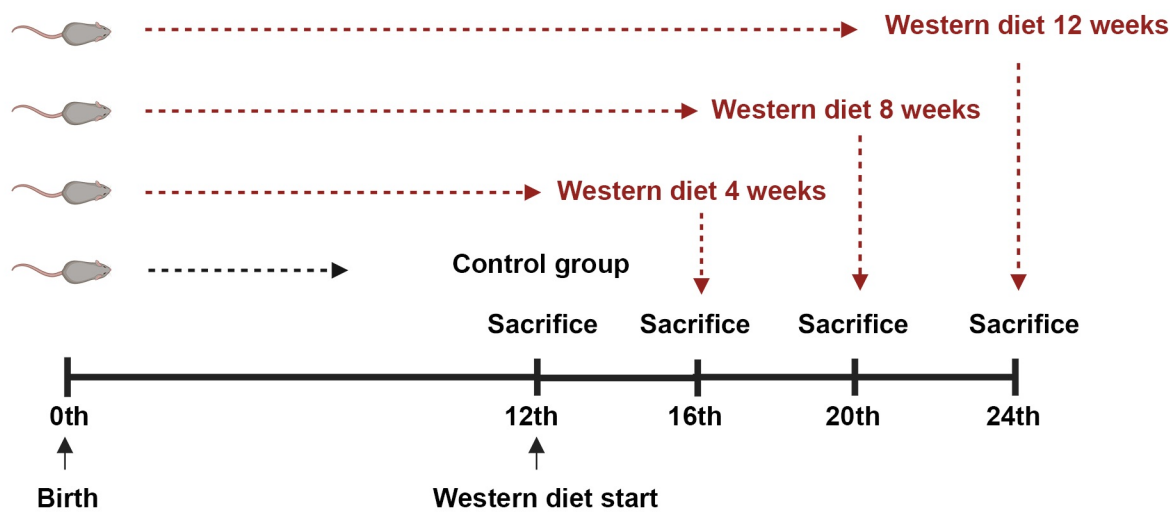


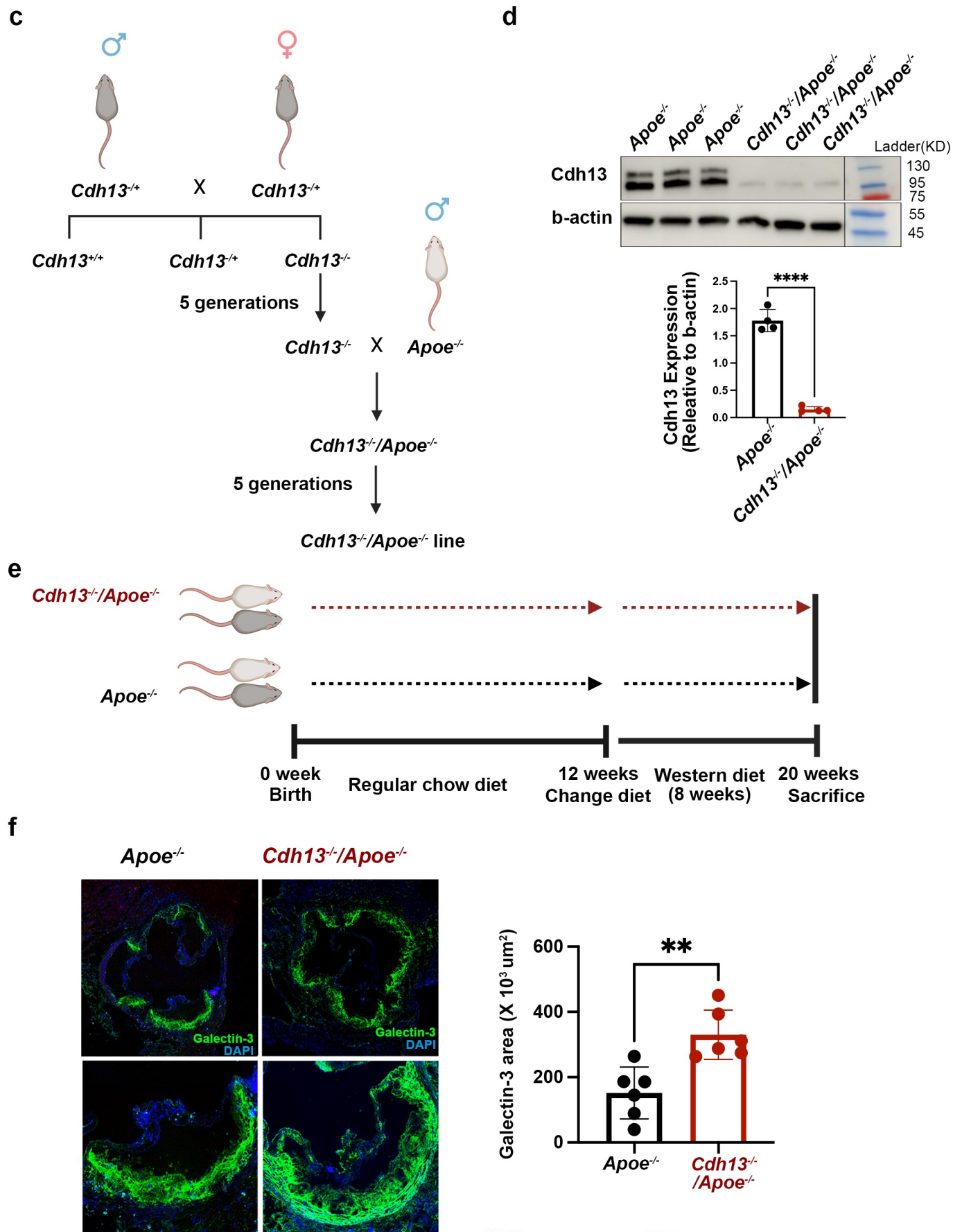
a



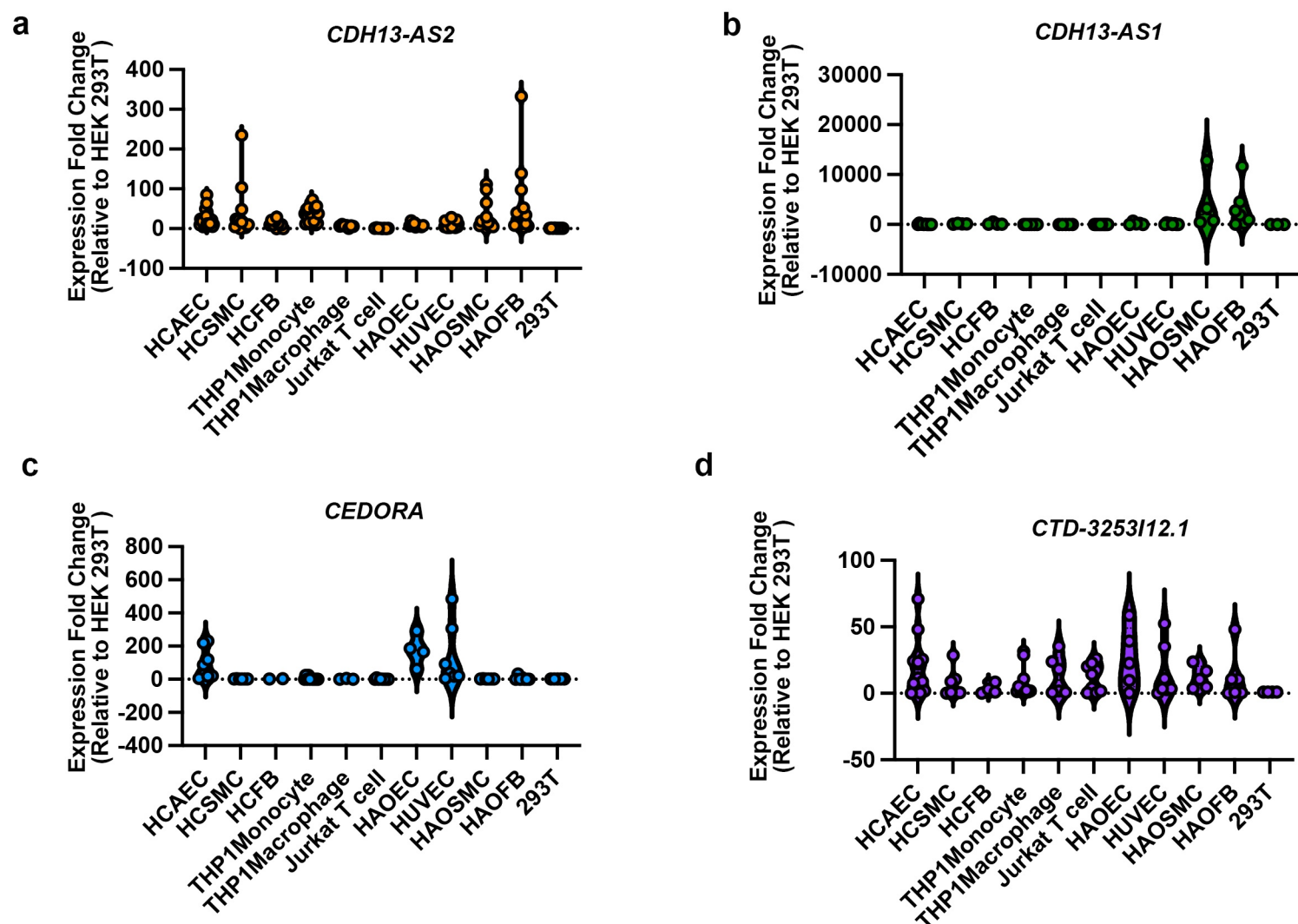
b



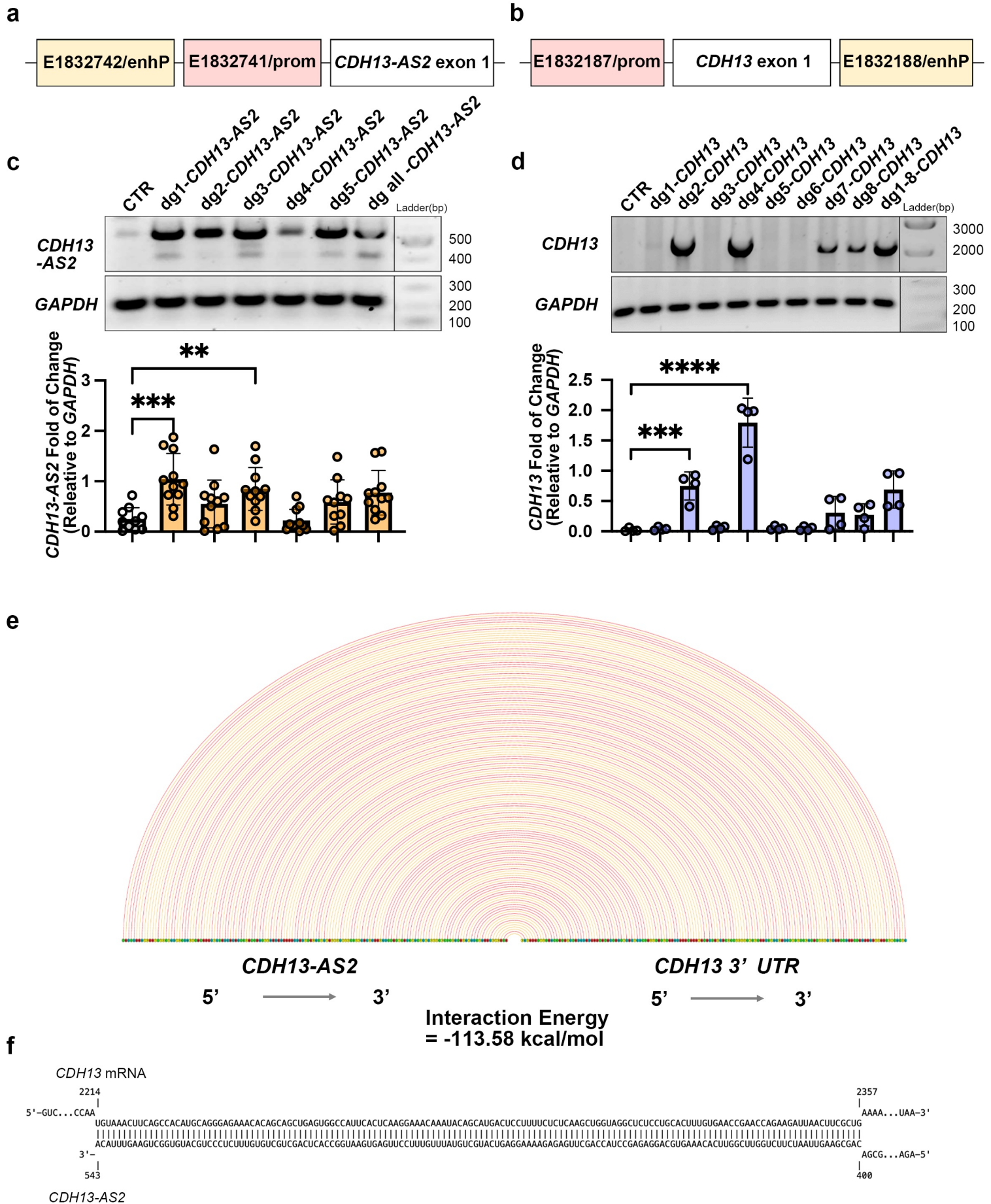
Extended Data Fig.1: The *CDH13* CAD GWAS locus (a) and experimental scheme of exploring *Cdh13* level during atherosclerosis development in mice. **a**, The locus zoom plot was made based on the latest summary genetic statistic of CAD GWAS from the CARDIoGRAMplusC4D Consortium(Fig.1a and 1b). **b**, Atherosclerosis development was induced in *Apoe*^{-/-} mice by weeks of Western diet feeding as indicated. Artery *Cdh13* protein level was evaluated according to the time points(Fig.1c).



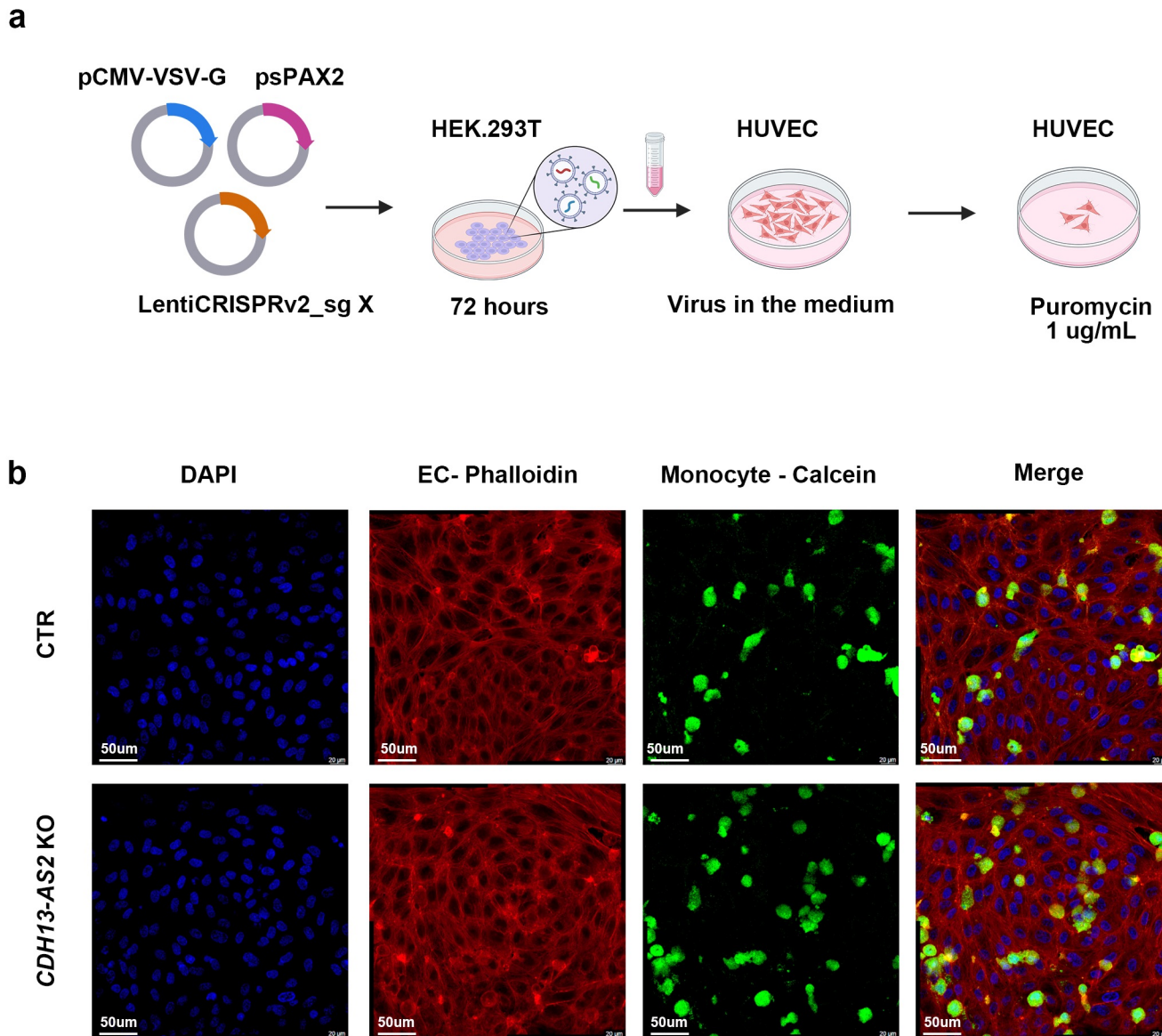
Extended Data Fig.1: The *CDH13* CAD GWAS locus and experimental scheme of exploring *Cdh13* level during atherosclerosis development in mice. **c**, Generation of *Cdh13*^{-/-}/*Apoe*^{-/-} transgenic mouse model(Fig.1e). **d**, Confirmation of *Cdh13* knockout by Western blotting of protein level in mouse aortic tissue(unpaired t-test, ****, $P \leq 0.0001$). **e**, The timeline to induce atherosclerosis phenotypes in transgenic mouse models(Fig.1e). **f**, In comparison to the *Apoe*^{-/-} mice, *Cdh13*^{-/-}/*Apoe*^{-/-} mice displayed increased leukocyte infiltration at the aortic roots marked by Galectin-3 staining. Unpaired t-test was used as the statistic method: **, $P \leq 0.01$;



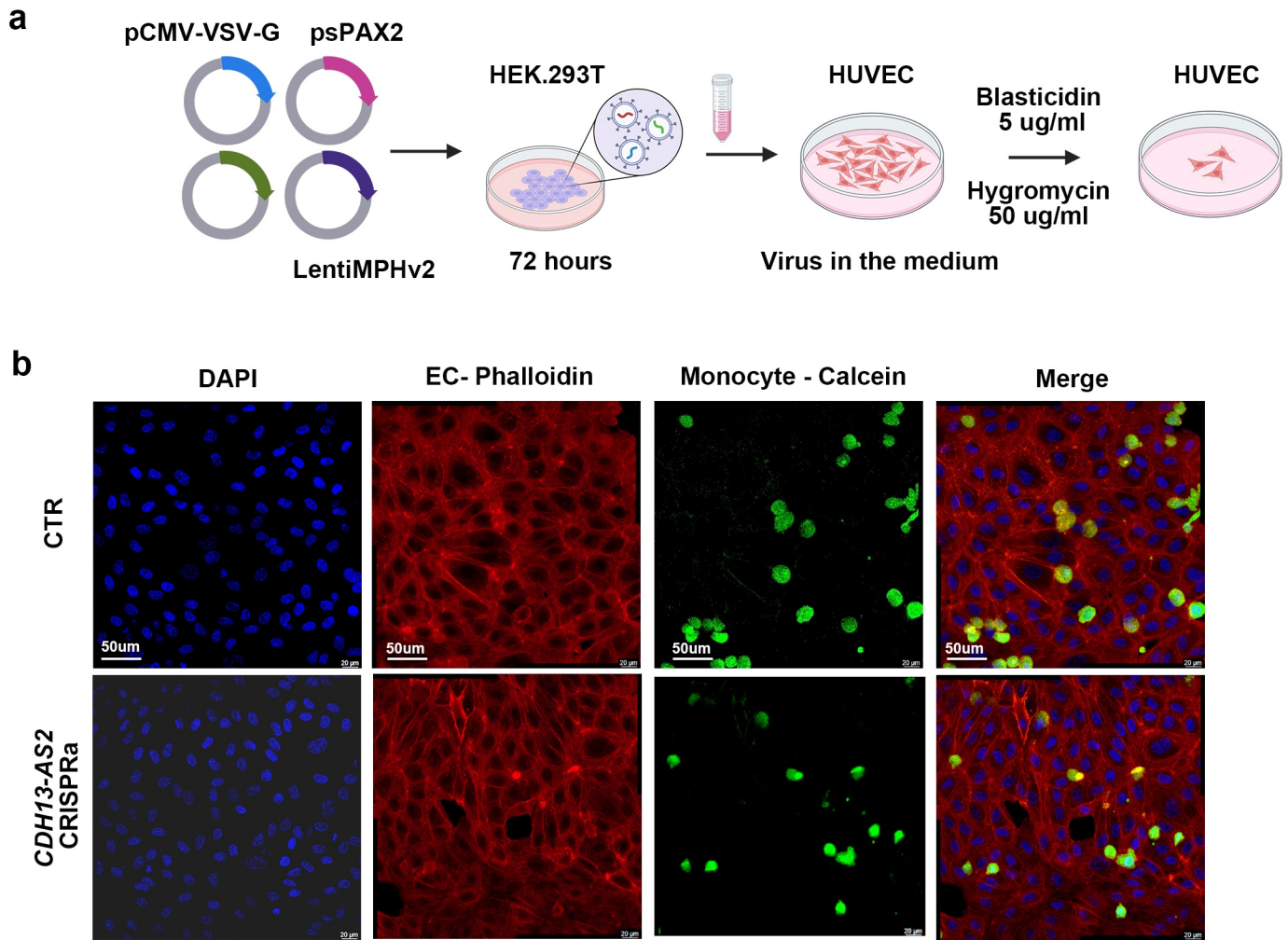
Extended Data Fig.2: The expression of lncRNAs in vascular cell types. **a** through **d**, lncRNAs expression in vascular cells. HUVECs, HAOEC, and HCAEC, human umbilical vein, aorta, and coronary artery endothelial cells; HAOSMC and HCSMC, human aorta and coronary artery smooth muscle cells; HCFB and HAOFB, human coronary artery and aorta fibroblasts; THP1, monocyte isolated from peripheral blood from an acute monocytic leukemia patient; macrophage, differentiated from THP1 via 100ng/ml phorbol 12-myristate 13-acetate (PMA) treatment for 72 hours; T cell, the immortalized line of human T lymphocyte cell, Jurkat. The four gene expressions were assessed by qPCR and the results were first normalized to GAPDH and then compared with HEK.293 T cells.



Extended Data Fig.3: The binding of *CDH13* and *CDH13-AS2* by prediction and CRISPR-based transcriptional activation (CRISPRa). **a,b**, ENCODE IDs and positions of targeted promoter (prom) and enhancer (enhP) of *CDH13-AS2* (**a**) and *CDH13* (**b**). **c**, For *CDH13-AS2*, five dgRNAs were tested individually or combined (dg1-5) (Ordinary one-way ANOVA multiple comparisons). **, $P \leq 0.01$; ***, $P \leq 0.001$. **d**, For *CDH13*, eight dgRNAs were tested individually or combined (dg1-8) (Ordinary one-way ANOVA multiple comparisons). ***, $P \leq 0.001$; ****, $P \leq 0.0001$. **e,f**, LncRRsearch webtool predicts the pair-wise interaction of *CDH13-AS2* with *CDH13* 3'UTR with a local base-pairing interaction energy of -113.58 kcal/mol.

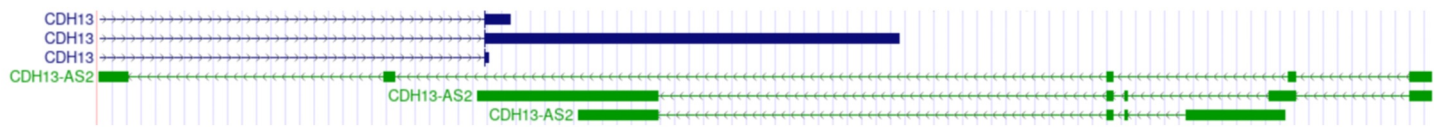


Extended Data Fig.4: Workflow of generation of CRISPR knockout HUVEC lines and full images of the adhesion assay of Fig.4g. a, HUVEC CRISPR knockout cell line generated by lentivirus treatment. **b**, Representative images of adhesion assay between control (CTR) and CDH13-AS2 KO HUVEC cells. HUVEC cells were labeled by phalloidin (red), TPH1 monocytes by calcein (green), and DNA by DAPI (blue).



Extended Data Fig.5: Workflow of generation of CRISPR-based transcriptional activation (CRISPRa) cell line and full images of the adhesion assay of Fig.5g. a, Workflow of CRISPRa in HUVEC cells. **b,** Representative images of adhesion assay between control (CTR) and CDH13-AS2 CRISPRa HUVEC cells. HUVEC cells were labeled by phalloidin (red), TPH1 monocytes by calcein (green), and DNA by DAPI (blue).

Basic Gene Annotation Set from GENCODE Version 47lift37 (Ensembl 113)



Extended Data Fig.6: The genomic position of *CDH13-AS2* and *CDH13* 3'UTR. The genome region of chr16:83,823,408-83,841,500 (GRCh37/hg19) was shown to visualize the full length of *CDH13-AS2*, *CDH13* 3'UTR, and the overlap of the two. Data was extracted from the UCSC Genome Browser on Human (GRCh37/hg19).